High Phenolics Rutgers Scarlet Lettuce Improves Glucose Metabolism in High Fat Diet-Induced Obese Mice

Diana M. Cheng[a], **Diana E. Roopchand**[a], **Alexander Poulev**[a], **Peter Kuhn**[a], **Isabel Armas**[a], **William D. Johnson**[c], **Andrew Oren**[a], **David Ribnicky**[a], **Ehud Zelzion**[b], **Debashish Bhattacharya**[b], and **Ilya Raskin**[a,*]

[a] Department of Plant Biology, Rutgers, The State University of New Jersey, New Brunswick, New Jersey, United States of America

[b] Department of Ecology, Evolution and Natural Resources, Rutgers, The State University of New Jersey, New Brunswick, New Jersey, United States of America

[c] Pennington Biomedical Research Center, Baton Rouge, Louisiana, United States of America

Abstract

Scope—The ability of high phenolic Rutgers Scarlet Lettuce (RSL) to attenuate metabolic syndrome and gut dysbiosis was studied in very high fat diet (VHFD)-fed mice. Phenolic absorption was assessed in vivo and in a gastrointestinal tract model.

Methods and results—Mice were fed VHFD, VHFD supplemented with RSL (RSL-VHFD) or store-purchased green lettuce (GL-VHFD), or low-fat diet (LFD) for 13 weeks. Compared to VHFD or GL-VHFD-fed groups, RSL-VHFD group showed significantly improved oral glucose tolerance ($p<0.05$). Comparison of VHFD, RSL-VHFD, and GL-VHFD groups revealed no significant differences with respect to insulin tolerance, hepatic lipids, body weight gain, fat mass, plasma glucose, triglycerides, free fatty acid, and lipopolysaccharide levels, as well as relative abundances of major bacterial phyla from 16S rDNA amplicon data sequences (from fecal and cecal samples). However, RSL and GL-supplementation increased abundance of several taxa involved in plant polysaccharide degradation/fermentation. RSL phenolics chlorogenic acid, quercetin-3-glucoside, and quercetin-malonyl-glucoside were bioaccessible in the TIM-1 digestion model, but had relatively low recovery.

Conclusions—RSL phenolics contributed to attenuation of postprandial hyperglycemia. Changes in gut microbiota were likely due to microbiota accessible carbohydrates in RSL and GL

rather than RSL phenolics, which may be metabolized, absorbed, or degraded before reaching the colon.

Keywords

Metabolic syndrome; phenolics; gut microbiota; lettuce; bioaccessibility

Introduction

Currently available drugs have been ineffective in curtailing the epidemic of metabolic syndrome (MetS) and its progression to type-2 diabetes (T2D), indicating a need for new therapeutic approaches. Epidemiological studies suggest that polyphenol-rich foods, such as fruits, vegetables, teas, and spices, provide resilience against chronic metabolic diseases [1,2]. Health organizations encourage higher consumption of plant-based foods and consumers are increasingly interested in consuming foods that provide health protective benefits beyond basic nutrition [3].

Rutgers Scarlet Lettuce (RSL) was developed using non-transgenic tissue culture methods to contain high levels of phenolic compounds relative to other lettuce varieties. Major phytochemicals in RSL include the phenolic, chlorogenic acid, and polyphenols quercetin malonyl-glucoside and cyanidin malonyl-glucoside, collectively referred to as phenolics [4], which have all been associated with attenuation of MetS in humans and rodent models. Chlorogenic acid-rich decaffeinated green coffee bean extract decreased post-prandial blood glucose levels in healthy subjects [5] and promoted weight loss in overweight volunteers [6]. Quercetin supplementation significantly decreased waist circumference, postprandial systolic blood pressure, and postprandial triacylglycerol concentrations in healthy males, which may contribute to modulating risk factors of cardiovascular disease [7,8]. Purified anthocyanin supplementation has been reported to reduce pro-inflammatory mediators [9] in healthy subjects as well as increase high-density lipoprotein (HDL)-cholesterol in healthy and dyslipidemic patients [10,11]. Oral administration of dehydrated RSL powder for eight days acutely reduced hyperglycemia and improved insulin sensitivity in very high fat diet (VHFD)-fed mice compared to vehicle control [4]. Oral administration of an aqueous extract of RSL for 28 days improved oral glucose tolerance and decreased total hepatic lipids compared to VHFD-fed control mice [12].

Phenolic compound bioavailability depends on structural characteristics and susceptibility to metabolism/degradation by host and gut microbes during gastrointestinal transit [13,14]. Chlorogenic acid was reportedly absorbed in the stomach and small intestine of rats with intact compound detectable in urine and plasma [15]; however, conflicting data have been reported regarding detection of intact chlorogenic in plasma in human studies [16,17]. Gut microbiota metabolize chlorogenic acid to bioavailable metabolites accounting for 60% of intake [18]. Plasma concentrations of anthocyanins and quercetin glucosides have been reported in the nanomolar range [19,20]. Although anthocyanins are degraded by digestive enzymes and microbes in the digestive tract, their metabolites were detected in millimolar concentrations in the gut lumen [19,20]. Recent data suggest that poorly absorbed grape or cranberry polyphenols attenuate symptoms of MetS/T2D in mice by modulating gut

microbiota community structure and promoting a bloom in *Akkermansia muciniphila,* a gut microbe associated with metabolic health [21,22].

We demonstrated that, compared to low phenolic green lettuce (GL), high phenolic RSL supplementation is more effective in attenuating symptoms of MetS/T2D in VHFD-fed C57BL/6J mice. In addition to evaluating metabolic health and gut microbiota in vivo, absorption of RSL phenolics was assessed in vivo and in vitro using the TNO Intestinal Model-1 (TIM-1) model of the human upper gastrointestinal (GI) tract.

Material and Methods

Materials

The following standards were purchased: sinapic acid, hippuric acid, caffeic acid, quercetin 3-glucoside (all 98% purity, Sigma, St. Louis, MO), chlorogenic acid (primary standard grade, 98% purity, Chromadex, Irvine, CA), and cyanidin 3-*O*-β-glucopyranoside (97% purity, Polyphenols, Norway). BeadBug™ Microtube Homogenizer and 3.0 mm zirconium beads were purchased from Benchmark Scientific (Edison, NJ).

RSL looseleaf variety NFR, was provided by Shamrock Seed Co. (Salinas, CA) and green leaf lettuce (GL) variety Crispa (Andy Boy, Salinas, CA) were purchased from the grocery store (Stop and Shop, Highland Park, NJ). NFR plant and seed vouchers were made and deposited at the Chrysler Herbarium and ATCC [4,12]. Outer leaves and tops of RSL lettuce heads were used as they have the highest levels of phenolics. Lettuce leaves were rinsed, lyophilized and homogenized in a Vitamix Professional 500 Blender (Cleveland, OH) to a fine powder. Dried RSL and GL powders were used for phytochemical extraction, nutritional analyses, and rodent diet formulations.

Phytochemical analysis

Six replicates of each lettuce variety, 0.5 g dried powder, were extracted with 15 mL of solvent (methanol:water:acetic acid; 85:14.5:0.5) three times as previously described [4]. Extract volumes were recorded and aliquots filtered through a 0.45 μm nylon syringe filter (Fisherbrand, Pittsburgh, PA) prior to analysis. Samples and standards were injected into UPLC-MS for quantification (see below). Chlorogenic acid, quercetin 3-glucoside and cyanidin 3-*O*-β-glucopyranoside were injected (1 μL) at 20, 500, and 1000 ng/μL to generate a linear calibration curve for quantification. UV peak area at absorption maxima of 325, 254, and 517 nm were used to quantify chlorogenic acid, quercetin glucosides and cyanidin glucosides, respectively.

TNO Intestinal Model-1 (TIM-1) experiments

Details of the TIM-1 model (TNO Triskelion, The Netherlands) have been described at length [23] (Supp. Methods). Three independent TIM-1 runs with RSL feeding were completed under fed state conditions to evaluate bioaccessibility of phenolics. RSL (cultivar NFR-S-4) was grown in Rutgers' greenhouse growth chamber as previously described [4]. Leaves of 2 - 3 month old RSL (40 g fresh wt.) were added to 200 mL of simulated stomach enzyme solution. Jejunal and ileal filtrates and ileal efflux were collected hourly.

Subsamples of TIM-1 filtrates (35 mL) were partitioned with chloroform (10 mL) and the aqueous layer was frozen at −80°C, lyophilized, and extracted in methanol:water:acetic acid, 85:15.5:0.5, as described for phytochemical analysis. TIM-1 was fed water as a control experiment to verify that compounds in filtrates and efflux samples did not originate from the porcine bile used in the TIM-1 model. Bioaccessibility is an indicator of bioavailability and is defined as the amount of compound released from a food matrix that can pass through jejunal and ileal membranes reflecting availability for intestinal absorption *in vivo*. Compounds captured in the ileal efflux represent theoretical colonic input and exposure to microbiota of the large intestine. Compounds collected in the residues are those that remained in the stomach, duodenum, jejunum, and ileum after the 4 h digestion. Recoveries of phenolics were calculated by dividing the amount collected in each compartment (jejunum and ileum filtrate, ileum effluent, and residue) by the total input from the fresh lettuce stomach solution.

UPLC-MS

Samples were analyzed by a UPLC/MS system including the Dionex® UltiMate 3000 RSLC ultra-high pressure liquid chromatography system as described in [24]. Substances were separated on a Phenomenex™ C8 reverse phase column, size 150×2 mm, particle size 3 μm, pore size 100 Å. The mobile phase consisted of 2 components: Solvent A (0.5% ACS grade acetic acid in double distilled de-ionized water, pH 3 - 3.5), and Solvent B (100% acetonitrile). For UPLC-MS/MS analysis of RSL and GL lyophilized powder extracts, the mobile phase flow was 0.20 mL/min, and an isocratic mode was used for the first 60 min of the separation with 11% B and 89% A mobile phase composition. From 60-71 min, a linear gradient from 11% B to 100% B was used, and the column allowed to wash for 4 min. During the subsequent 5 min the mobile phase composition was brought back to initial conditions linearly. For UPLC/MS analysis of plasma metabolites and TIM filtrates, the mobile phase flow was 0.20 mL/min, and a gradient mode was used for analyses. The initial conditions of the gradient were 95% A and 5% B; the solvent system was brought to 5% A and 95% B over 30 min and kept for the next 8 min, and during the subsequent 4 min the ratio was brought to initial conditions. An 8-10 min equilibration interval was included between subsequent injections. The average pump pressure using these parameters was typically around 4000-4300 psi for the initial conditions.

Rodent diet formulations

Phytochemical analysis of lettuce varieties showed RSL had a greater content of all phenolics compared to GL (Table 1). Samples of RSL and GL powders were sent for proximate analysis (New Jersey Feed Labs, Trenton, NJ) and information was used to formulate very high fat diet (VHFD; 60% kcal from fat, D12492, Research Diets, New Brunswick, NJ) containing 6.4% (w/w) of RSL or GL powder. VHFD supplemented with RSL (RSL-VHFD) provided chlorogenic acid, quercetin glucosides and cyanidin glucosides at 2 mg/g diet (0.2% w/w each, a total of 0.61%). VHFD supplemented with GL (GL-VHFD) provided chlorogenic acid and quercetin malonyl glucoside at 0.06 mg/g diet (0.006% w/w each, a total of 0.012%). RSL-VHFD, GL-VHFD and VHFD were isocaloric, delivering equivalent amounts of macronutrients (Table S1). On a caloric basis, RSL and GL provided 4.2% kcal and 4.1% kcal, respectively. A low fat diet (LFD; 10% kcal from fat,

D12450J, Research Diets, New Brunswick, NJ) was included as an additional control, providing equivalent amounts of sucrose as VHFD over same caloric intake.

Animal care and procedures

Animal experiments were approved by the Internal Animal Care and Use Committee at Rutgers, The State University of New Jersey (# 04-023). Sixty mice (5 week-old, male, C57BL/6J) were purchased from Jackson Labs (Bar Harbor, ME) and acclimatized to the animal facilities for one week with *ad libitum* access to water and chow diet (Purina, #5015) prior to experiments. Mice were initially housed 5 mice to a cage and maintained at 25 °C on a 12 h light/dark cycle. Six week-old mice were randomly divided into body weight-balanced groups (3 mice per cage, 5 cages per diet group) and provided LFD, VHFD, RSL-VHFD, or GL-VHFD (n = 15 mice per diet group) for 13 weeks.

Body composition measurements (fat mass, lean mass, free water, and total water masses) were evaluated by Echo-MRI™ (Houston, TX) at 0, 4, and 11 weeks of feeding. At weeks 5 and 9 oral glucose tolerance tests (OGTT) were performed. At week 8 an oral maltose tolerance test (OMTT) was performed. Mice were fasted for 6 h, then given a glucose or maltose challenge (2 g/kg) and blood glucose was measured every 30 min over 120 min. Insulin sensitivity was evaluated after 12 weeks. Mice were fasted for 4 h prior to an insulin injection (0.7 U/kg) and blood glucose was recorded every 30 min over 120 min. The percent change in blood glucose was calculated by: $100 * [\text{Glucose}_n - \text{Glucose}_{initial}] / (\text{Glucose}_{initial})$, where n refers to the 30, 60, 90, or 120 min time points.

At the end of 13 weeks, mice were fasted for 4 h and euthanized by CO_2 asphyxiation and decapitation. Gastrocnemius muscle, epididymal fat and liver were collected into cryovials. Lumen of intestinal tissue segments (jejunum, ileum, colon) were flushed with cold saline to remove feces and cleaned tissues were collected in cryovials. All samples were snap frozen in liquid nitrogen, and stored at −80 °C for RNA and protein analyses.

Trunk blood was collected into tubes containing EDTA (BD, Franklin Lakes, NJ) centrifuged for 10 min at $1000 \times g$ (within the first 30 min) and plasma was collected and stored at −20 °C. Plasma was sent to Pennington Biomedical Research Center (PBRC, Baton Rouge, LA) for biochemical analysis of glucose, insulin, triglycerides, free fatty acids, and lipopolysaccharide (LPS) concentrations, as previously described [12,21,25].

Plasma metabolite analysis

Samples for plasma metabolite analysis were prepared in triplicate as described by Stalmach et al. [26] (Supp. Methods). Sinapic acid was not detected in a pooled sample of plasma from the RSL supplementation group, and was therefore used as an internal control. Solutions were analyzed by UPLC-MS as described above (5 μL injections) and standards of sinapic acid, hippuric acid, caffeic acid, and chlorogenic acid were used to generate a calibration curve by determining UV peak areas at 227 nm for hippuric acid and 324 nm for the other three phenolic acids. To calculate metabolite recovery efficiency, 1 μg of sinapic acid, hippuric acid, caffeic acid, and chlorogenic acid were added to an independent set of

plasma samples from mice on VHFD. Percent recovery = (μg of compound recovered in sample) / (μg of compound added to sample) * 100.

Statistical analysis of mouse phenotypes

Statistically significant differences among groups were determined using a general linear model analysis of variance. Analysis of variance was performed to obtain a global test of differences among treatment groups. Longitudinal data from ITT and OGTT were analyzed by applying a mixed effects model for repeated measures across 120 min. *Post-hoc* analyses (Tukey or Tukey-Kramer tests) were performed to assess significance ($\alpha = 0.05$) between time points. Means labeled with different letters indicate significant differences. Statistical procedures were performed with SAS 9.3 software (Cary, NC).

16S rDNA gene sequencing and analysis

Small unit (16S) rDNA gene sequencing was performed on cecal and fecal samples collected after 13 weeks on experimental diets. Fecal samples collected from mice housed in the same cage (n = 3 mice per cage, 5 cages per diet group) were pooled resulting in 5 fecal samples per diet group. Cecal samples from individual mice were processed separately. DNA extraction cecal data was obtained for a subset of mice in each diet group (LFD, n = 9; VHFD, n = 6; RSL-VHFD, n = 9; GL-VHFD, n = 5). Genomic DNA was extracted using the PowerSoil bacterial DNA extraction kit (MoBio, Carlsbad CA) and cleaned using Nucleospin gDNA clean-up columns (Machery-Nagel). The V3-V4 region of 16 rDNA gene was amplified according to Illumina protocols using forward primer 5'-TCGTCGGCAGCGTCAGATGTGTATAAGAGACAGCCTACGGGNGGCWGCAG and reverse primer 5'-GTCTCGTGGGCTCGGAGATGTGTATAAGAGACAGGACTACHVGGGTATCTAA TCC. The following thermocycler protocol was used: denature at 95 °C for 3 min, 25 cycles of 95 °C for 30 s, 60 °C for 30 s, and 72 °C for 30 s, with a final extension at 72 °C for 5 min. Amplification reactions for each sample were confirmed by 1.5% gel electrophoresis and amplicons were then cleaned with Ampure XP kit (Agencourt, Danvers, MA). A second Index PCR using Nextera XT Index kit v2, set D primers (Illumina cat# FC-131-2004) was performed to attach Illumina dual-index barcodes and sequencing adaptors with following thermocycler protocol: denature at 95 °C for 3 min, 5 cycles of 95°C for 30 sec, 55 °C for 30 sec, and 72°C for 30 sec, with a final extension at 72 °C for 5 min. Libraries were cleaned with Ampure XP kit and quantified using the Quant-iT Picogreen ds DNA Assay Kit (Invitrogen, Carlsbad, CA). Barcoded amplicons from all 49 samples were pooled (4 nM) and paired-end sequencing was performed on an Illumina MiSeq instrument using MiSeq kit MS-102-3003 (600-cycle) and 5% phiX for quality control. Due to poor quality reverse reads only the forward reads were used in subsequent analyses. Sequences were demultiplexed and dual indexing barcodes were removed. Forward read FastQ files were processed with Trimmomatic-0.33 to remove Illumina adaptor sequences and low quality bases (sliding window mode) while retaining sequences of at least 180 bp. FastQC was run on untrimmed and trimmed sequences to verify sequence quality before and after trimming. QIIME (v 1.9.1) script multiple_extract_barcodes.py was used to strip primer sequence from trimmed forward reads followed by multiple_split_libraries_fastq.py. The resulting seqs.fna

file was input into vsearch 1.8.1 to perform dereplication, removal of singletons, OTU (operational taxonomic units) clustering to centroids, and chimera detection using uchime_denovo. A Python script was used to calculate the number of OTU centroids. Using vsearch, the seqs.fna file was mapped to centroids with a threshold of 97% identity and the resulting .uc file was converted into an OTU table (.txt), which was then converted into json biom format with the biom convert function. QIIME was used to assign taxonomy to representative sets of OTUs using the default database (97_otu_taxonomy.txt). Sequences in the representative set of OTUs were aligned using PyNAST, filtered and used to build a phylogenetic tree. Bray-Curtis principal coordinate analysis was performed using the QIIME script "beta_diversity_through_plots.py." Statistical analyses of microbial community structure (permutational multivariate ANOVA [PERMANOVA] and analysis of similarities [ANOSIM]) were done using the QIIME script "compare_categories.py." *Post-hoc* analysis was performed with Statistica v9 (StatSoft). Microbial biomarker discovery was performed using the LEfSe algorithm (35), with an LDA score 3 set as the threshold for significance [27].

Results

Food intake, body weight, body composition, liver lipids, and plasma biochemistry

Mice consuming RSL-VHFD, GL-VHFD, or VHFD (i.e. VHFD-based groups) initially consumed more calories compared to mice on the LFD, but by the end of the first week the average caloric intake was not significantly different among all four diet groups for the duration of the experiment (Fig. 1A). Over the 13 weeks, mice in all VHFD-based groups gained significantly more body weight than LFD (Fig. 1B), specifically, more fat mass (Fig. 2A), compared to LFD-fed mice. RSL or GL supplementation did not attenuate body mass or fat mass accumulation induced by VHFD (Fig 1B, Fig 2A). Mean lean mass was not significantly different between all four diet groups, except at week 11 where the GL-VHFD group was greater than LFD-fed mice (Fig. 2B).

Compared to VHFD alone, RSL or GL supplementation did not result in significant differences in liver mass, liver lipids, liver lipid accumulation scores, plasma glucose, insulin, and free fatty acids (Tables S2 and S3); however, all VHFD-based groups were different compared to LFD group. The four diet groups did not show significantly different levels of plasma triglycerides (Table S3).

Carbohydrate metabolism and insulin sensitivity

Oral glucose tolerance tests (OGTT) with glucose challenge were performed after 5 and 9 weeks on experimental diets. Mice in the LFD group served as a control for normal glucose metabolism (Fig 3). At weeks 5 and 9, mean fasting blood glucose levels (time = 0 min) trended higher in all VHFD-based groups compared to the LFD group, demonstrating the hyperglycemic effects of VHFDs (Fig. 3A, B). At 5 weeks the RSL-VHFD and GL-VHFD groups showed significant differences in oral glucose tolerance compared to mice on VHFD, as determined by area under the blood glucose response curve (Fig. 3A). At 9 weeks, the RSL-VHFD group had significantly better oral glucose tolerance than both GL-VHFD and VHFD groups, which did not significantly differ in glucose metabolism (Fig. 3B).

As polyphenols have also been demonstrated to reduce glucose uptake through the inhibition of disaccharide hydrolysis [28,29], glucose tolerance in response to an oral maltose challenge was tested at 8 weeks. At 30 min, blood glucose levels of mice supplemented with RSL or GL were not significantly different than the LFD-fed group, which was significantly lower than that observed for the VHFD (Fig. 3C). Area under the blood glucose response curve was significantly reduced in both RSL and GL-supplemented groups compared to VHFD.

Compared to LFD, insulin sensitivity was significantly attenuated in all VHFD based groups and compared to VHFD, the response to insulin was not significantly improved in mice fed RSL or GL supplemented diet (Fig. S1). As the insulin tolerance test did not suggest RSL phenolics potentiate insulin activity, animals were not given insulin injections prior to euthanasia.

Polyphenol supplementation was reported to stimulate glucose transport by activating Akt and AMPK cell signaling pathways in metabolic tissues [30-32]. Protein was extracted from liver, muscle, and adipose tissue for western blot analysis of AMPK and Akt activation by phosphorylation. VHFD-based groups did not show significantly different levels of AMPK or Akt phosphorylation (Supp. methods). Additionally, RNA extracted from ileum tissue showed no significant difference in relative TNFα gene expression between RSL-VHFD (0.90 ± 0.24) and VHFD (1.02 ± 0.22) groups (mean ± SD) (Supp. methods).

Gut microbiota analysis

The 16S rDNA gene sequencing of cecal and fecal samples indicated microbial communities were strongly impacted by the different diets (PERMANOVA; F= 7.0; $p< 0.001$). Cecal and fecal samples from the same diet groups clustered together (Fig. 4A). Bray-Curtis principal coordinate analysis showed that the three VHFD-based groups separated from LFD along PC2, explaining 17.4% of the variation (Fig. 4A). RSL and GL supplemented groups clustered together and separated from both VHFD and LFD groups along PC1, explaining an additional 22.0% of variation (Fig. 4A).

To avoid pseudoreplication, additional analyses on cecal and fecal subsets were performed separately. Analysis of bacterial relative abundance showed that, as previously reported [21], gut microbial communities of mice fed a LFD were dominated by bacteria from the Firmicutes and Bacteroidetes (Fig. 4B), whereas all VHFD-based groups had significantly increased proportion of Firmicutes versus Bacteroidetes (Fig. 4C, Kruskal-Wallis ANOVA and multiple comparisons test). Compared to the VHFD control, supplementation with RSL showed a trend toward decreasing the ratio of Firmicutes to Bacteroidetes, whereas supplementation with GL did not show this effect (Fig. 4C). Differences in the relative abundances of Verrucomicrobia, Proteobacteria, Actinobacteria or Tenericutes between the four diet groups were non-significant (Fig. 4B, Kruskal-Wallis ANOVA and multiple comparisons test, $p > 0.05$).

To reveal distinguishing microbial biomarkers of RSL or GL supplementation in fecal and cecal samples, linear discriminant analysis was performed using the LEfSE algorithm [27] on OTU abundance data generated at all taxonomic levels (Table S4). Both RSL and GL-

supplemented mice showed significant increases in specific taxa within the family *Lachnospiraceae* (order Clostridiales), which include several butyrate-producing microbes [33]. *Roseburia* spp. (*Lachnospiraceae* family) and *Ruminococcus* spp. (*Ruminococcaceae* family) were significantly increased in both fecal and cecal samples of RSL-supplemented mice, but not in GL samples (Table S4). *Ruminococcus* spp. are capable of degrading resistant starches and *Roseburia* spp. ferment plant polysaccharides to produce butyrate [34]. The *Peptococcaceae* family known to oxidize butyrate [35] was also increased in RSL samples. Cecal and fecal samples of the GL group, but not RSL group, showed increased levels of several butyrate-producing taxa including *Coprococcus, Blautia*, and *Moryella* spp. within the *Lachnospiraceae* family and *Clostridium* spp. within the *Ruminococcaceae* family [34] (Table S4).

Plasma phenolic metabolites

Hippuric acid was detected in plasma of RSL-VHFD and GL-VHFD fed mice, but not in plasma of VHFD mice. Other major phenolics and metabolites including, chlorogenic acid, caffeic acid, quinic acid, cinnamic acid, protocatechuic acid, ferulic acid, vanillic acid, benzoic acid, dicaffeoylquinic acids, gallic acid, or quercetin and cyanidin glucosides were not detected by selective ion monitoring in plasma of RSL or GL supplemented mice. However, presence of metabolites may not have been detected if levels were below instrument sensitivity; for chlorogenic acid, a 5 ng injection was clearly detectable. Plasma samples were spiked with sinapic acid as an internal standard. Recovery of an internal spike of sinapic acid from plasma of LFD, VHFD, RSL-VHFD, and GL-VHFD groups was 53.3 $\pm$ 4.2%, 55.6 $\pm$ 9.2%, 46.1 $\pm$ 3.9%, and 52.1 $\pm$ 1.6% (mean $\pm$ SD), respectively. The mean plasma concentration of hippuric acid in RSL-VHFD group was 7.5 $\pm$ 6.9 μM, thus, accounting for recovery, the estimated concentration may be up to 15 μM. Hippuric acid levels in plasma from the GL-VHFD group was not within the limits of quantification.

Bioaccessibility of RSL phenolics

Bioaccessible compounds are those that can pass through jejunal and ileal membranes and are potentially available for intestinal absorption. Chlorogenic acid, quercetin 3-glucoside, and quercetin malonyl-glucoside were bioaccessible in the TIM-1 model as compounds were recovered from the jejunal and ileal filtrates, whereas cyanidin glucosides were not bioaccessible as they were not detected (Fig. 5). The greatest amount of chlorogenic acid bioaccessible was 0.8 μmol in the jejunum and 0.32 μmol in the ileum (Fig. 5A). The greatest amount of quercetin 3-glucoside bioaccessible was 0.63 μmol in the jejunum and 0.12 μmol in the ileum (Fig. 5B). The greatest amount of quercetin malonyl-glucoside bioaccessible was 1.17 μmol in the jejunum and 0.36 μmol in the ileum (Fig. 5C). There was a wide variation for quercetin malonyl-glucoside due to its instability, which may have contributed to greater than expected levels of its breakdown product, quercetin 3-glucoside. The highest concentration of chlorogenic acid, quercetin 3-glucoside, and quercetin malonyl glucoside were 3.2 $\pm$ 1.0 μM, 2.5 $\pm$ 0.2 μM, 4.6 $\pm$ 4.3 μM, respectively, in the jejunum, and 1.27 $\pm$ 0.47 μM, 0.47 $\pm$ 0.14 μM, and 1.44 $\pm$ 1.26 μM, respectively, in the ileum.

Calculation of total recovery of RSL phenolics from the intake amount showed that 4.5% of chlorogenic acid and 7.5% of quercetin malonyl-glucoside was recovered, indicating that

they were not stable through the digestive process (Table 2). In comparison, quercetin 3-glucoside recovery was 20.1% and likely due to quercetin malonyl-glucoside breakdown, as quercetin 3-glucoside was lower than quercetin malonyl-glucoside content in RSL plant material (Table 1). Cyanidin glucosides were not bioaccessible and only 0.3% was detected in the residue of the jejunum and ileum (Table 2).

Discussion

Mice fed RSL-VHFD demonstrated significantly improved glucose metabolism compared to mice fed VHFD or GL-VHFD after 9 weeks on the experimental diets (Fig 3B). However, other physiological parameters: insulin tolerance, hepatic lipids, body weight gain, fat mass, plasma glucose, triglycerides, free fatty acid, and lipopolysaccharide levels were not significantly different between VHFD groups.

Using the TIM-1 model of human digestion, chlorogenic acid, quercetin 3-glucoside, and quercetin malonyl-glucoside were bioaccessible, but their overall recovery was rather low, 4.5% and 7.5%, respectively, and in micromolar concentrations (**Table 2**); the native compounds were not detected in any plasma samples. Low recoveries of total phenolics after intestinal digestion were also reported from kale (6.8%) [36]. In another study, chlorogenic acid was degraded by 40-70%, after intestinal digestion [37]. Results were consistent with data showing that native phenolic forms are rarely detected in plasma because they undergo modifications by host enzymes and gut bacteria [38].

In this study, hippuric acid was the only phenolic metabolite quantifiable in plasma of RSL-supplemented mice. Hippuric acid is a product of microbial metabolism of phenolic in the colon [39,40] and was the major plasma and urinary metabolite in rats supplemented with chlorogenic, caffeic, or quinic acids whereas these parent compounds were not detected [18]. Chlorogenic acid was reported to be absorbed intact in rat stomach [15,41]; however, chlorogenic acid is mainly hydrolyzed in the small intestine by microbial esterases and products, such as hippuric acid, are then absorbed in the colon [15,41,42]. Chlorogenic acid was shown to suppress hepatic gluconeogenesis [12], possibly by the absorbed compound and metabolites being delivered to liver via the portal vein [38]. We hypothesized that the anti-hyperglycemic effects of RSL may be, at least partially, explained by the presence of chlorogenic acid and related metabolites. Further research may focus on the specific activity of phenolic metabolites.

In this study, mice consumed rodent diet providing an average of 400 kcal/kg body weight of which 16 kcal (4%) were from RSL or GL. Lettuce provides 19 kcal per 84 g (2 cups); this is equal to 70 g fresh lettuce per kg mouse body weight. For an 80 kg human, this would be 5600 g fresh lettuce. Accounting for the faster metabolism of rodent vs. human (by 10-fold), we estimate an intake of 560 g of fresh lettuce for humans. In this mouse study, lettuce is the only vegetable source of phenolics, which is unusual for a human diet. Direct correlation from murine models to humans is difficult, as differences including form of intake, time/duration of intake, additional dietary components, interspecies metabolic and bioavailability differences, are obvious limitations in rodent models.

As previously reported, VHFD induced an increase in the ratio of Firmicutes to Bacteroidetes compared to LFD feeding [21]. Compared to the VHFD group, GL-supplementation did not reduce the Firmicutes to Bacteroidetes ratio; however, supplementation with phenolic-rich RSL showed a trend of reducing this ratio (Fig. 5C). Significant differences at the phyla level were not observed between diet groups. The main effect of RSL or GL supplementation, as determined by LEfSE analysis, was increased abundance of taxa associated with digestion of plant polysaccharides. RSL and GL induced increased levels of taxa within families *Ruminococcaceae*, *Lachnospiraceae*, and *Peptococcaceae*, which are involved in plant polysaccharide degradation [34], fermentation of monosaccharides to butyrate [33], and butyrate oxidation [35], respectively (Supp. Table S4).

In contrast to the present study, Etxerberria *et al.* found that quercetin supplementation of rats fed a high fat and sucrose diet significantly reduced the Firmicutes to Bacteroidetes ratio and increased the abundance of *A. muciniphila* in the gut [43]. Interrogation of the public data from the Human Microbiome Project and MetaHIT found no simple association between obesity and phylum level shifts in human microbiota [44]; however, HFD feeding consistently increased the ratio of Firmicutes to Bacteroidetes in the C57BL/6 mouse model of metabolic syndrome. *In vivo* data suggests that quercetin glucosides, present in RSL, are more efficiently absorbed in the small intestine compared to quercetin aglycone [45] and therefore may be less likely to impact the gut microbiota community. A plausible explanation for this difference is that the glycoside form can more efficiently penetrate the intestinal mucus layer, followed by deglycosylation by β-glucosidases near the brush border and subsequent absorption of the resulting aglycone through the epithelium [46]. Hydrophobic quercetin aglycone would be less able to infiltrate the mucus layer and instead enter the colon for metabolism by gut bacteria [46].

Previous studies showed that mice fed HFD supplemented with Concord grape or cranberry polyphenols [21,22] demonstrated anti-diabetic effects, while significantly reducing Firmicutes to Bacteroidetes ratio and increasing intestinal abundance of *A. muciniphila.* We hypothesize that poorly bioavailable and poorly digestible grape and cranberry polyphenols that reach the colon, specifically high molecular weight proanthocyanidins [47], are likely responsible for this bloom in *A. muciniphila*. Proanthocyanidins are strong antioxidants that may scavenge reactive oxygen species in the dysbiotic GI tract, promoting the growth of beneficial obligate anaerobes, such as *A. muciniphila*, while suppressing less favorable facultative anaerobes. Proanthocyanidins are poorly metabolized by gut bacteria [46], a property that could explain a strong antioxidant effect in the gut. In contrast to proanthocyanidins, the phenolic compounds present in RSL are more readily absorbed, metabolized, or degraded, which could explain their modest effects on the cecal and fecal gut microbiota. This offers an intriguing possibility that relatively bioavailable and digestible vegetable phenolics and poorly bioavailable / digestible berry phenolics improve glucose metabolism through two different mechanisms – systemically, via liver gluconeogenesis, for the former and via gut microbiome for the later.

Author Manuscript

Supplementary Material

Refer to Web version on PubMed Central for supplementary material.

Acknowledgements

Abbreviations

|	
GL	green lettuce
LFD	low fat diet
LPS	lipopolysaccharide
MetS	metabolic syndrome
OTU	operational taxonomic units
RSL	Rutgers Scarlet Lettuce
T2D	type-2 diabetes
VHFD	very high fat diet

References

1. Muraki I, Imamura F, Manson JE, Hu FB, et al. Fruit consumption and risk of type 2 diabetes: results from three prospective longitudinal cohort studies. BMJ. 2013; 347:f5001. [PubMed: 23990623]

2. Cooper AJ, Forouhi NG, Ye Z, Buijsse B, et al. Fruit and vegetable intake and type 2 diabetes: EPIC-InterAct prospective study and meta-analysis. Eur. J. Clin. Nutr. 2012; 66:1082–1092. [PubMed: 22854878]

3. Bigliardi B, Galati F. Innovation trends in the food industry: The case of functional foods. Trends Food Sci.Technol. 2013; 31:118–129.

4. Cheng DM, Pogrebnyak N, Kuhn P, Krueger CG, et al. Development and phytochemical characterization of high polyphenol red lettuce with anti-diabetic properties. PLoS ONE. 2014; 9:e91571. [PubMed: 24637790]

5. Blum J, Lemaire B, Lafay S. Effect of a green decaffeinated coffee extract on glycemia – a pilot prospective clinical study. Nutrafoods. 2007; 6:13–17.

6. Dellalibera O, Lemaire B, Lafay S. Svetol®, a decaffeinated green coffee extract, induces weight loss and increases the lean to fat ratio in overweight volunteers. Phytothér Expér. 2006; 4:194–197.

7. Pfeuffer M, Auinger A, Bley U, Kraus-Stojanowic I, et al. Effect of quercetin on traits of the metabolic syndrome, endothelial function and inflammation in men with different APOE isoforms. Nutr. Metab. Cardiovasc. Dis. 2013; 23:403–409. [PubMed: 22118955]

8. Russo M, Spagnuolo C, Tedesco I, Bilotto S, Russo GL. The flavonoid quercetin in disease prevention and therapy: Facts and fancies. Biochem. Pharmacol. 2012; 83:6–15. [PubMed: 21856292]

9. Karlsen A, Retterstøl L, Laake P, Paur I, et al. Anthocyanins inhibit nuclear factor-κB activation in monocytes and reduce plasma concentrations of pro-inflammatory mediators in healthy adults. J. Nutr. 2007; 137:1951–1954. [PubMed: 17634269]

10. Hassellund SS, Flaa A, Kjeldsen SE, Seljeflot I, et al. Effects of anthocyanins on cardiovascular risk factors and inflammation in pre-hypertensive men: a double-blind randomized placebo-controlled crossover study. J. Hum. Hypertens. 2013; 27:100–106. [PubMed: 22336903]

11. Qin Y, Xia M, Ma J, Hao Y, et al. Anthocyanin supplementation improves serum LDL- and HDL-cholesterol concentrations associated with the inhibition of cholesteryl ester transfer protein in dyslipidemic subjects. Am. J. Clin. Nutr. 2009; 90:485–492. [PubMed: 19640950]

12. Cheng DM, Pogrebnyak N, Kuhn P, Poulev A, et al. Polyphenol-rich Rutgers Scarlet Lettuce improves glucose metabolism and liver lipid accumulation in diet induced obese C57BL/6 mice. Nutrition. 2014; 30:S52–S58. [PubMed: 24985107]

13. Manach C, Williamson G, Morand C, Scalbert A, Rémésy C. Bioavailability and bioefficacy of polyphenols in humans. I. Review of 97 bioavailability studies. Am. J. Clin. Nutr. 2005; 81:230S–242S. [PubMed: 15640486]

14. Kemperman RA, Bolca S, Roger LC, Vaughan EE. Novel approaches for analysing gut microbes and dietary polyphenols: Challenges and opportunities. Microbiol.-SGM. 2010; 156:3224–3231.

15. Lafay S, Gil-Izquierdo A, Manach C, Morand C, et al. Chlorogenic acid is absorbed in its intact form in the stomach of rats. J. Nutr. 2006; 136:1192–1197. [PubMed: 16614403]

16. Stalmach A, Steiling H, Williamson G, Crozier A. Bioavailability of chlorogenic acids following acute ingestion of coffee by humans with an ileostomy. Arch. Biochem. Biophys. 2010; 501:98–105. [PubMed: 20226754]

17. Farah A, Monteiro M, Donangelo CM, Lafay S. Chlorogenic acids from green coffee extract are highly bioavailable in humans. J. Nutr. 2008; 138:2309–2315. [PubMed: 19022950]

18. Gonthier M, Verny M, Besson C, Rémésy C, Scalbert A. Chlorogenic acid bioavailability largely depends on its metabolism by the gut microflora in rats. J Nutr. 2003; 133:1853–1859. [PubMed: 12771329]

19. Williamson G. Possible effects of dietary polyphenols on sugar absorption and digestion. Mol. Nutr. Food Res. 2013; 57:48–57-57. [PubMed: 23180627]

20. Williamson G, Manach C. Bioavailability and bioefficacy of polyphenols in humans. II. Review of 93 intervention studies. Am. J. Clin. Nutr. 2005; 81:243S–255S. [PubMed: 15640487]

21. Roopchand DE, Carmody RN, Kuhn P, Moskal K, et al. Dietary polyphenols promote growth of the gut bacterium Akkermansia muciniphila and attenuate high-fat diet-induced metabolic syndrome. Diabetes. 2015; 64:2847–2858. [PubMed: 25845659]

22. Anhê FF, Roy D, Pilon G, Dudonné S, et al. A polyphenol-rich cranberry extract protects from diet-induced obesity, insulin resistance and intestinal inflammation in association with increased Akkermansia spp. population in the gut microbiota of mice. Gut. 2015; 64:872–883. [PubMed: 25080446]

23. Lila MA, Ribnicky DM, Rojo LE, Rojas-Silva P, et al. Complementary approaches to gauge the bioavailability and distribution of ingested berry polyphenolics. J. Agric. Food Chem. 2012; 60:5763–5771. [PubMed: 22111523]

24. Cheng DM, Kuhn P, Poulev A, Rojo LE, et al. In vivo and in vitro antidiabetic effects of aqueous cinnamon extract and cinnamon polyphenol-enhanced food matrix. Food Chem. 2012; 135:2994–3002. [PubMed: 22980902]

25. Roopchand DE, Kuhn P, Rojo LE, Lila MA, Raskin I. Blueberry polyphenol-enriched soybean flour reduces hyperglycemia, body weight gain and serum cholesterol in mice. Pharmacol. Res. 2013; 68:59–67. [PubMed: 23220243]

26. Stalmach A, Mullen W, Barron D, Uchida K, et al. Metabolite profiling of hydroxycinnamate derivatives in plasma and urine after the ingestion of coffee by humans: Identification of biomarkers of coffee consumption. Drug Metab.d Dispos. 2009; 37:1749–1758.

27. Segata N, Izard J, Waldron L, Gevers D, et al. Metagenomic biomarker discovery and explanation. Genome Biol. 2011; 12:1–18.

28. Adisakwattana S, Lerdsuwankij O, Poputtachai U, Minipun A, Suparpprom C. Inhibitory Activity of Cinnamon Bark Species and their Combination Effect with Acarbose against Intestinal alpha-

glucosidase and Pancreatic alpha-amylase. Plant Foods Hum. Nutr. 2011; 66:143–148. [PubMed: 21538147]

29. Shihabudeen HMS, Priscilla DH, Thirumurugan K. Cinnamon extract inhibits alpha-glucosidase activity and dampens postprandial glucose excursion in diabetic rats. Nutr. Metab. 2011; 8:46.

30. Gannon NP, Conn CA, Vaughan RA. Dietary stimulators of GLUT4 expression and translocation in skeletal muscle: A mini-review. Mol. Nutr. Food Res. 2014; 59:48–64. [PubMed: 25215442]

31. Kawabata K, Mukai R, Ishisaka A. Quercetin and related polyphenols: New insights and implications for their bioactivity and bioavailability. Food Funct. 2015; 6:1399–1417. [PubMed: 25761771]

32. Ong KW, Hsu A, Tan BK. H. Chlorogenic acid stimulates glucose transport in skeletal muscle via AMPK activation: A contributor to the beneficial effects of coffee on diabetes. PLOS ONE. 2012; 7:e32718. [PubMed: 22412912]

33. Meehan CJ, Beiko RG. A phylogenomic view of ecological specialization in the Lachnospiraceae, a family of digestive tract-associated bacteria. Genome Biol. Evol. 2014; 6:703–713. [PubMed: 24625961]

34. Rajili -Stojanovi M, de Vos WM. The first 1000 cultured species of the human gastrointestinal microbiota. FEMS Microbiol. Rev. 2014; 38:996–1047. [PubMed: 24861948]

35. Vital M, Howe AC, Tiedje JM. Revealing the bacterial butyrate synthesis pathways by analyzing (meta)genomic data. mBio. 2014; 5:e00889–14. [PubMed: 24757212]

36. Kaulmann A, André CM, Schneider Y, Hoffmann L, Bohn T. Carotenoid and polyphenol bioaccessibility and cellular uptake from plum and cabbage varieties. Food Chem. 2016; 197(Part A):325–332. [PubMed: 26616956]

37. Bouayed J, Deußer H, Hoffmann L, Bohn T. Bioaccessible and dialysable polyphenols in selected apple varieties following in vitro digestion vs. their native patterns. Food Chem. 2012; 131:1466–1472.

38. D'Archivio M, Filesi C, Varì R, Scazzocchio B, Masella R. Bioavailability of the polyphenols: Status and controversies. Int. J. Mol. Sci. 2010; 11:1321–1342. [PubMed: 20480022]

39. DuPont MS, Bennett RN, Mellon FA, Williamson G. Polyphenols from alcoholic apple cider are absorbed, metabolized and excreted by humans. J. Nutr. 2002; 132:172–175. [PubMed: 11823574]

40. Nieman DC, Gillitt ND, Knab AM, Shanely RA, et al. Influence of a polyphenol-enriched protein powder on exercise-induced inflammation and oxidative stress in athletes: A randomized trial using a metabolomics approach. PLoS ONE. 2013; 8:e72215. [PubMed: 23967286]

41. Lafay S, Morand C, Manach C, Besson C, Scalbert A. Absorption and metabolism of caffeic acid and chlorogenic acid in the small intestine of rats. Br. J. Nutr. 2006; 96:39–46. [PubMed: 16869989]

42. Olthof MR, Hollman PCH, Katan MB. Chlorogenic acid and caffeic acid are absorbed in humans. J. Nutr. 2001; 131:66–71. [PubMed: 11208940]

43. Etxeberria U, Arias N, Boqué N, Macarulla MT, et al. Reshaping faecal gut microbiota composition by the intake of trans-resveratrol and quercetin in high-fat sucrose diet-fed rats. J. Nutr. Biochem. 2015; 26:651–660. [PubMed: 25762527]

44. Finucane MM, Sharpton TJ, Laurent TJ, Pollard KS. A taxonomic signature of obesity in the microbiome? Getting to the guts of the matter. PLoS ONE. 2014; 9:e84689. [PubMed: 24416266]

45. Morand C, Manach C, Crespy V, Remesy C. Respective bioavailability of quercetin aglycone and its glycosides in a rat model. Biofactors. 2000; 12:169–174. [PubMed: 11216481]

46. Gonzales GB, Van Camp J, Smagghe G, Raes K, Mackie A. Flavonoid–gastrointestinal mucus interaction and its potential role in regulating flavonoid bioavailability and mucosal biophysical properties. Food Res. Int. In press. doi:10.1016/j.foodres.2015.12.023.

47. Ou K, Gu L. Absorption and metabolism of proanthocyanidins. J. Funct. Foods. 2014; 7:43–53.
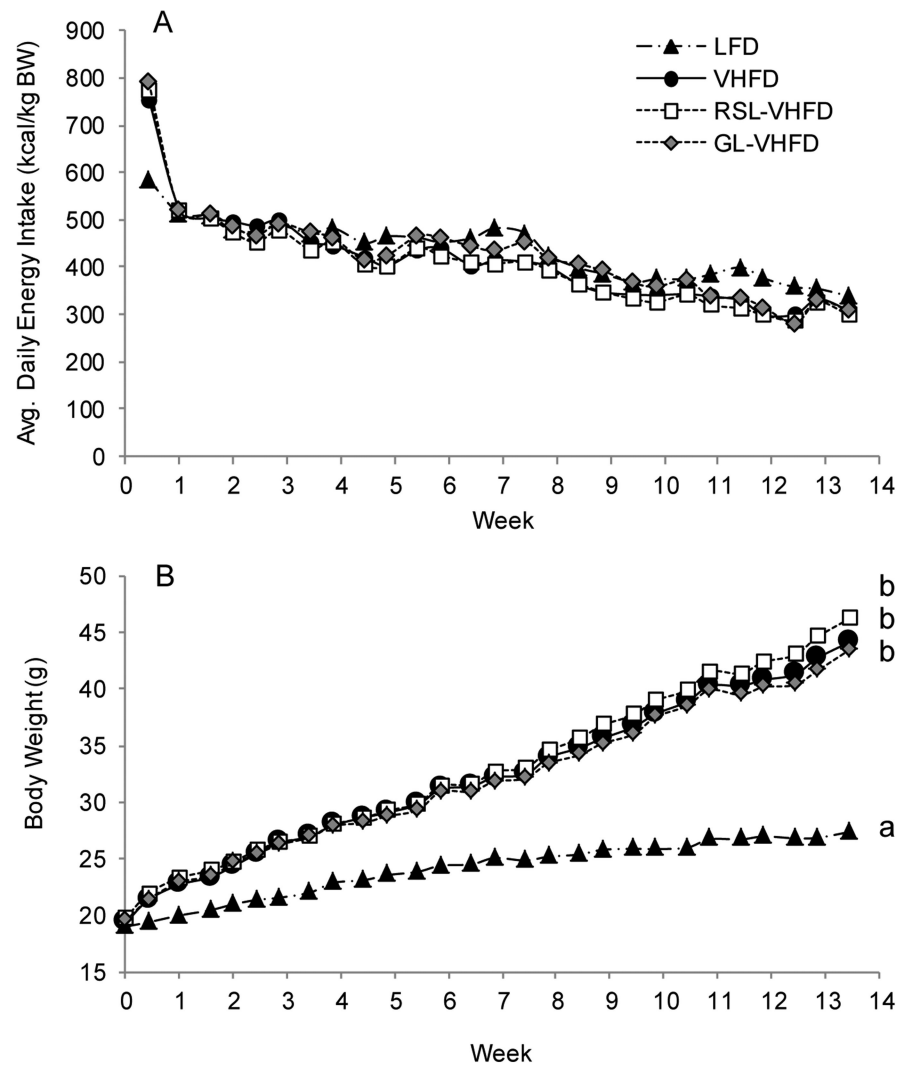
Figure 1.
RSL or GL supplementation did not affect body weight gain. Mean daily energy intake (A) and mean body weight (B) of mice on LFD, VHFD, Rutgers Scarlet Lettuce-supplemented VHFD (RSL-VHFD), and green lettuce-supplemented VHFD (GL-VHFD). Significant differences between treatments were determined by ANOVA and Tukey-Kramer post-hoc tests. Letters that are similar indicate no significant difference ($p > 0.05$).
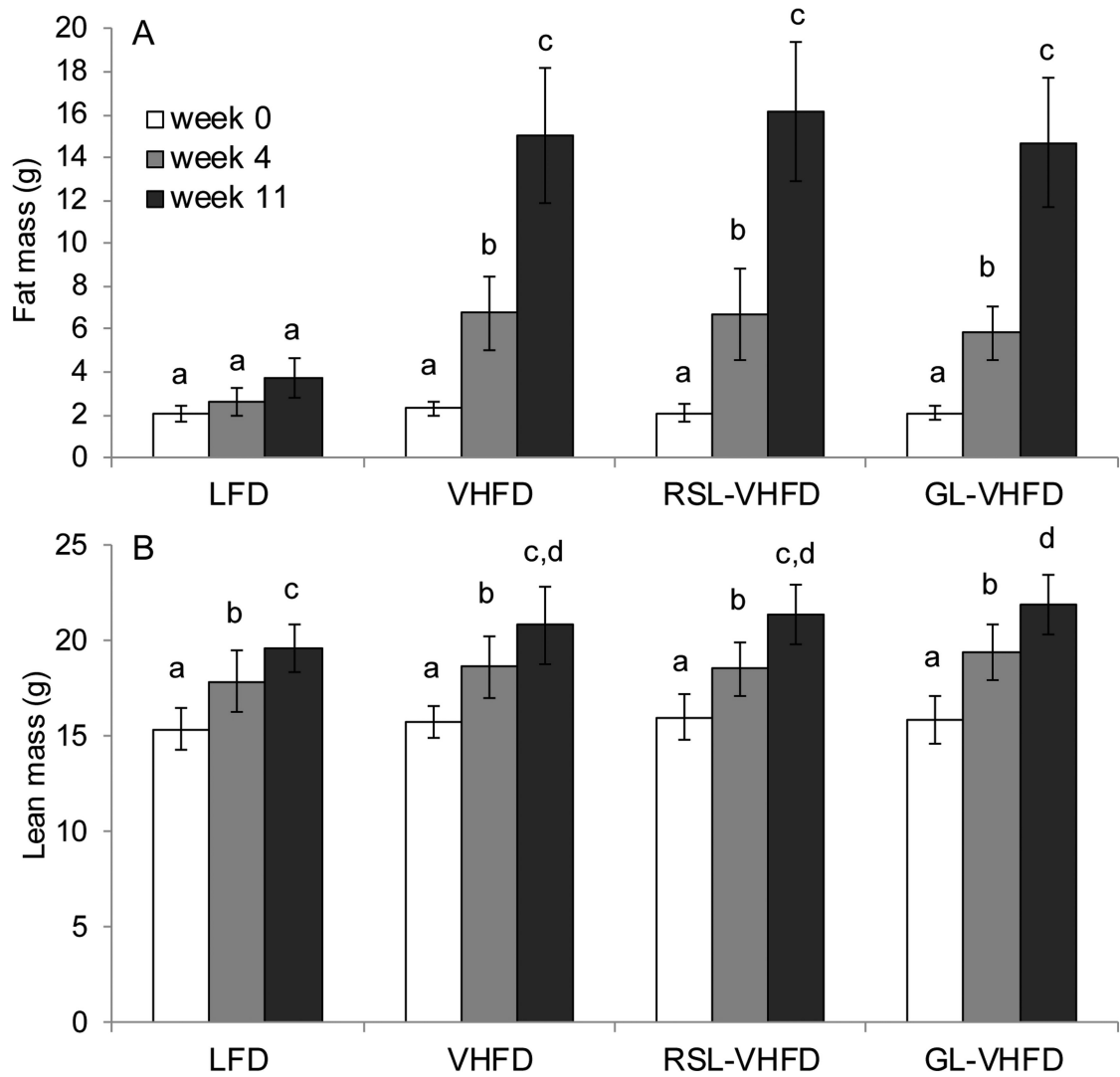
Figure 2.
RSL or GL supplementation did not affect fat or lean mass gain. Mean fat mass (A) and lean mass (B) of mice at 0, 4, and 11 weeks of experimental diets (Mean ± SD). Significant differences between diet groups at each time point were determined by ANOVA and Tukey-Kramer post-hoc tests. Letters that are similar indicate no significant difference ($p > 0.05$).
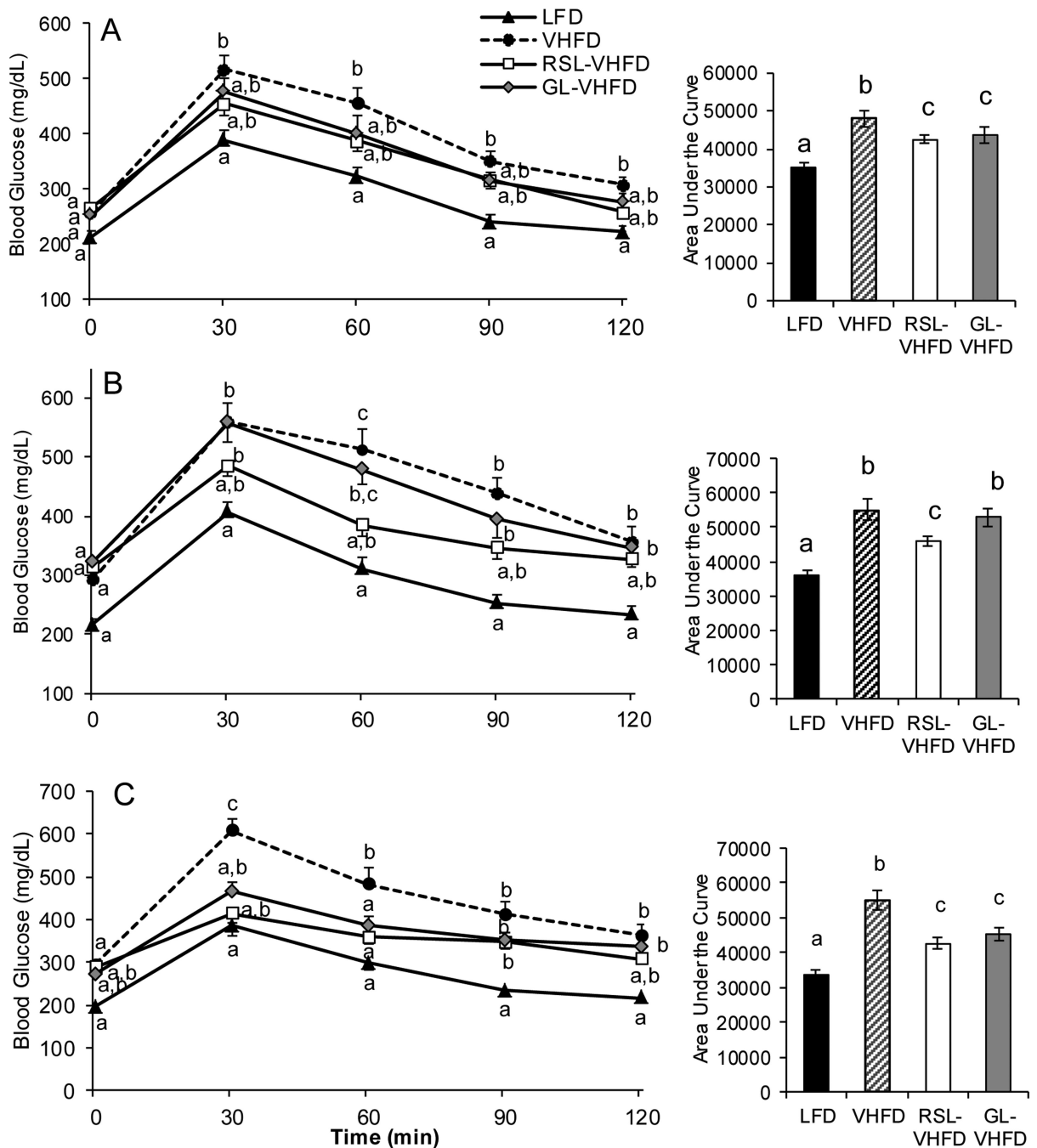
Figure 3.
RSL supplementation improved oral glucose tolerance after 9 weeks. Effects on glucose metabolism were evaluated by oral glucose tolerance tests at week 5 (A) and week 9 (B) post-supplementation. Effects on maltose/glucose metabolism evaluated was by oral maltose tolerance test (mice given a maltose challenge) after 8 weeks of experimental diets (C). In each case, blood glucose levels and corresponding areas under the curve (AUC) are shown. Differences in blood glucose at individual time points as well as differences in AUC values
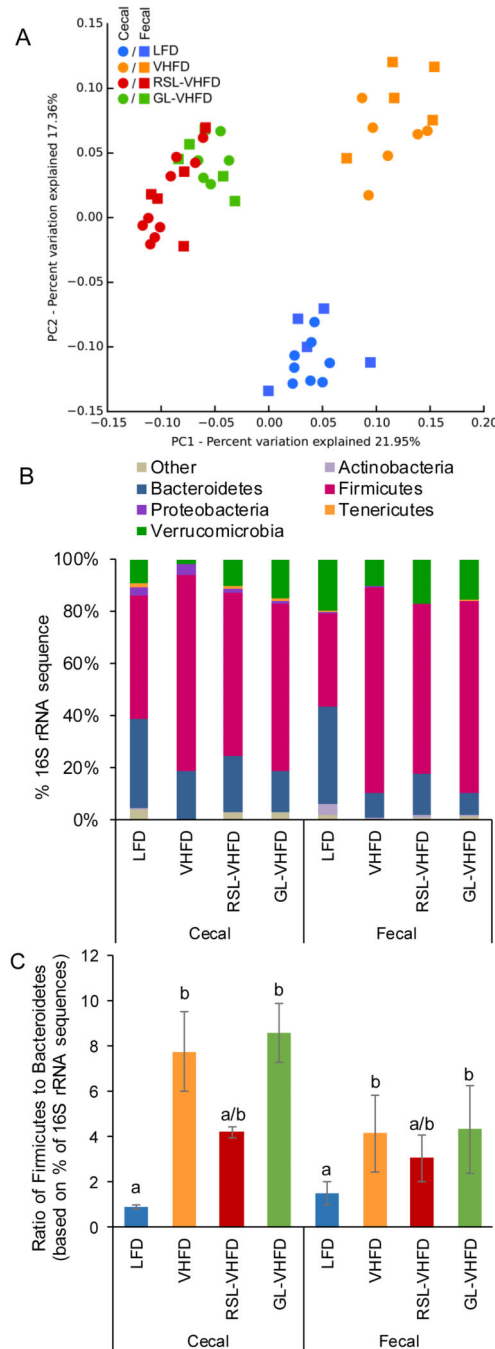
between the four diet groups were determined by ANOVA and Tukey post-hoc tests. Letters that are similar are not significantly different ($p > 0.05$).
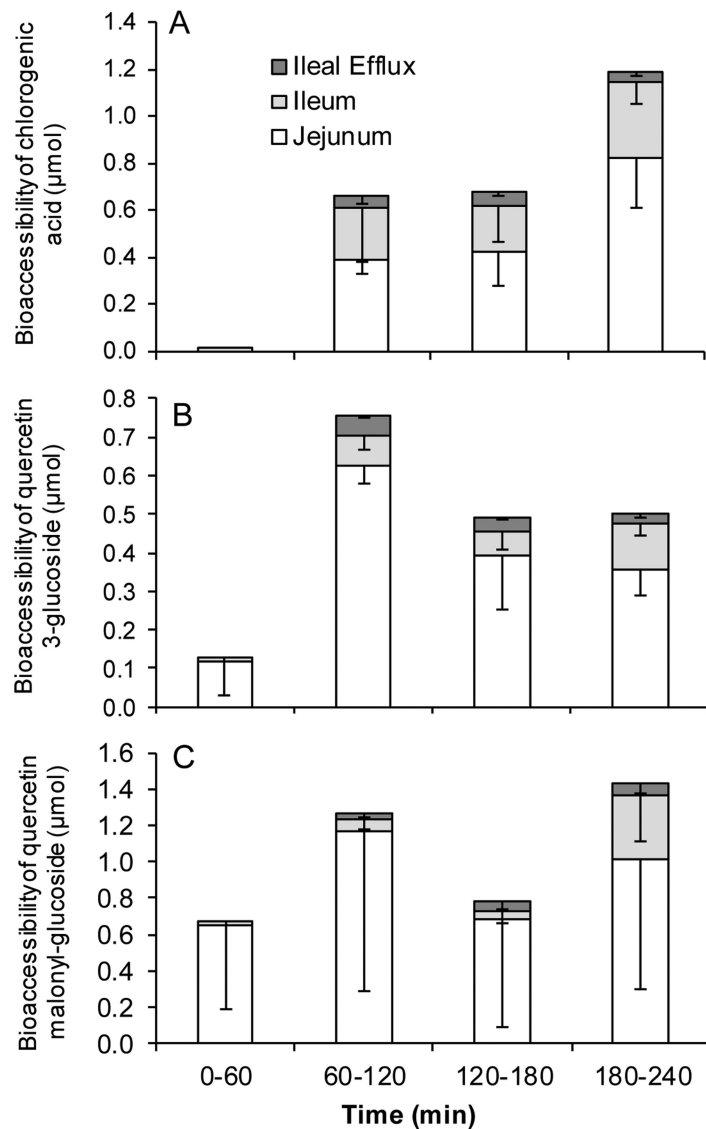
Figure 4.
Effect of RSL and GL supplementation on gut microbiota. (A) Principal coordinate analysis of 16S rDNA coding regions in cecal samples and fecal samples collected from mice after 13 weeks of consuming indicated diets. The RSL-VHFD and GL-VHFD samples formed distinct clusters when compared to the VHFD and LFD samples along PC1, accounting for 22% of variation in the sample pool. All VHFD based samples (RSL-VHFD, GL-VHFD, and VHFD) were separated from LFD along PC2, accounting for an additional 17% of variation. (B) RSL-VHFD, GL-VHFD, and VHFD groups were not different in relative

abundance of bacterial phyla in both cecal and fecal samples (Kruskal-Wallis ANOVA and multiple comparisons test; $p > 0.05$). (C) Ratio of the percentage 16S rDNA amplicons assigned to Firmicutes and Bacteroidetes. Compared to VHFD, only LFD samples showed a significantly lower Firmicutes to Bacteroidetes ratio (mean $\pm$ SEM) (Kruskal-Wallis ANOVA and multiple comparisons test, letters that are similar indicate no significant difference, $p > 0.05$).

Figure 5.
RSL phenolics are bioaccessible in TIM-1 model. RSL was introduced to TIM-1 in fed state. Chlorogenic acid (A), quercetin 3-glucoside (B), and quercetin malonyl-glucoside (C) bioaccessibility (mean ± SD of 3 independent runs) as a percent of input was determined in filtrates collected from jejunum, ileum, and efflux compartments at 1, 2, 3 and 4 h after start of digestion. Phenolics were quantified by UPLC-UV.

Table 1

Phenolic content of lettuces powders and lettuce supplemented diets (mean ± SD).

	RSL	GL	RSL	GL
	mg/g DW lettuce		mg/g diet	
Chlorogenic acid	31.1 ± 1.1	0.9 ± 0.0	2.0	0.06
Quercetin 3-glucoside	2.1 ± 0.1	-	0.1	
Quercetin malonyl-glucoside	29.8 ± 0.7	0.9 ± 0.0	1.9	0.06
Cyanidin 3-glucoside	0.6 ± 0.1	-	0.0	
Cyanidin malonyl-glucoside	33.4 ± 0.6	-	2.1	
Total polyphenols	78 ± 3.47	11 ± 1.5	5.0	0.7
Trolox equivalence	3083 ± 233	744 ± 214	197	48

Red lettuce: protein 27.3%, carbohydrate 47.7%, fat 3.7%, and fiber 7.8%

Green lettuce: protein 18.4%, carbohydrate 56.6%, fat 2.6%, and fiber 7.4%

Table 2

Bioaccessibility of Rutgers Scarlet Lettuce phenolics (mean ± SD).

	Chlorogenic acid	Quercetin 3-glucoside	Quercetin malonyl-glucoside
μmol			
Total jejunum + ileum filtrate	2.39 ± 0.52	1.76 ± 0.08	3.99 ± 2.83
Total ileum effluent	0.14 ± 0.05	0.12 ± 0.02	0.16 ± 0.12
Total residue	2.74 ± 1.76	0.86 ± 0.35	1.72 ± 1.51
Recovery	5.26 ± 2.26	2.74 ± 0.44	5.88 ± 4.27
% of input			
Total jejunum + ileum filtrate	1.97 ± 0.49	12.85 ± 1.31	5.12 ± 3.62
Total ileum effluent	0.12 ± 0.04	0.88 ± 0.22	0.21 ± 0.15
Total residue	2.43 ± 1.49	6.39 ± 2.82	2.21 ± 1.93
Recovery	4.51 ± 1.95	20.12 ± 4.26	7.54 ± 5.48